Analytical Expression of Non-Steady-State Concentrations and Current Pertaining to Compounds Present in the Enzyme Membrane of Biosensor

ARTICLE *in* THE JOURNAL OF PHYSICAL CHEMISTRY A · MAY 2011

Impact Factor: 2.69 · DOI: 10.1021/jp200520s · Source: PubMed

3 AUTHORS, INCLUDING:

Shanmugarajan Anitha

10 PUBLICATIONS **32** CITATIONS

SEE PROFILE

Lakshmanan Rajendran

Sethu Institute of Technology

135 PUBLICATIONS **409** CITATIONS

SEE PROFILE

THE JOURNAL OF PHYSICAL CHEMISTRY A

ARTICLE

pubs.acs.org/JPCA

Analytical Expression of Non-Steady-State Concentrations and Current Pertaining to Compounds Present in the Enzyme Membrane of Biosensor

Anitha Shanmugarajan,[†] Subbiah Alwarappan,[‡] and Lakshmanan Rajendran*[,†]

[†]Department of Mathematics, The Madura College, Madurai 625011, India

[‡]Nanotechnology Research and Education Center, University of South Florida, Tampa, Florida 33620-5350, United States

ABSTRACT: A mathematical model of trienzyme biosensor at an internal diffusion limitation for a non-steady-state condition has been developed. The model is based on diffusion equations containing a linear term related to Michaelis−Menten kinetics of the enzymatic reaction. Analytical expressions of concentrations and current of compounds in trienzyme membrane are derived. An excellent agreement with simulation data is noted. When time tends to infinity, the analytical expression of non-steady-state concentration and current approaches the steady-state value, thereby confirming the validity of the mathematical analysis. Furthermore, in this work we employ the complex inversion formula to solve the boundary value problem.

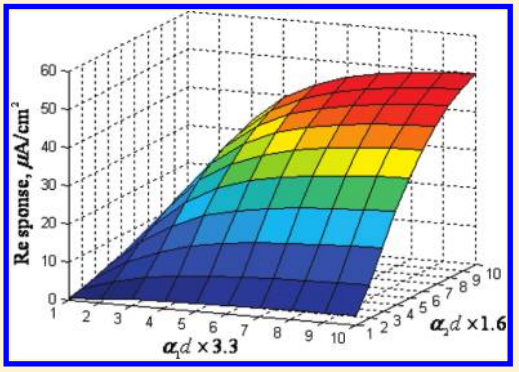

INTRODUCTION

Biosensors are analytical devices that combine the selectivity and specificity of an immobilized biologically active compound with a signal transducer.[1−3] The study of biosensors is of immense interest to optimize various analytical characteristics.[4−8] The thickness of the enzyme membrane has a considerable effect on the biosensor response as well as on the response time.[9,10] Practical biosensors that consist of a multilayer enzyme membrane,[11] with the model biosensors containing the exploratory monolayer membrane, are useful tools to study the biochemical behavior of biosensors.[12] Biosensors find immense applications in several fields, and this includes in routine clinical glucose monitoring,[13] in agriculture and the food processing industry,[14] and in the pharmaceutical industry.[15]

Earlier, analytical expressions pertaining to the steady-state concentrations and current of compounds in trienzyme membrane for all diffusion modules were calculated by Kulys.[16] However, to the best of our knowledge, no analytical expressions pertaining to the non-steady-state concentrations and current of compounds for all diffusion modules $\alpha_1 d$, $\alpha_2 d$, and $\alpha_3 d$ in a trienzyme membrane have been reported. The purpose of this article is to arrive at analytical expressions corresponding to non-steady-state concentrations and currents of compounds in trienzyme membrane for all diffusion modules using the complex inversion method.

MATHEMATICAL FORMULATION OF THE BOUNDARY VALUE PROBLEM

In a creatinine biosensor, initially the hydrolyzed creatinine reacts with creatininase (E_1) producing creatine (P_1) and then the hydrolyzed creatine reacts with creatinase (E_2) producing sacrosine (P_2). Following this, the oxidation of sacrosine will be carried out using sarcosine oxidase (E_3) to yield hydrogen peroxide (P_3). A general scheme that represents the reaction occurring at a creatinine biosensor is shown below:

$$S \xrightarrow{E_1} P_1 \xrightarrow{E_2} P_2 \xrightarrow{E_3} P_3 \qquad (1)$$

Here the rate of each reaction (V_i) is considered by the standard enzyme parameters $V_{max(i)}$ and $K_{m(i)}$, where $i = 1, 2$, and 3 for E_1, E_2, and E_3 catalyzed processes, respectively. $V_1 = V_{max(1)}s_1/K_{m(1)}$, $V_2 = V_{max(2)}p_1/K_{m(2)}$, and $V_3 = V_{max(3)}p_2/K_{m(3)}$, where s_1, p_1, and p_2 represent the concentrations of S, P_1, and and P_2 at concentrations less than the Michaelis−Menten constants ($K_{m(i)}$). The diffusion equations with a constant diffusion coefficient corresponding to the enzymatic conversion at a non-steady-state condition can be represented by eqs 2−5.[16]

$$\frac{1}{D}\frac{\partial s_1}{\partial t} = \frac{\partial^2 s_1}{\partial x^2} - \alpha_1{}^2 s_1 \qquad (2)$$

$$\frac{1}{D}\frac{\partial p_1}{\partial t} = \frac{\partial^2 p_1}{\partial x^2} + \alpha_1{}^2 s - \alpha_2{}^2 p_1 \qquad (3)$$

$$\frac{1}{D}\frac{\partial p_2}{\partial t} = \frac{\partial^2 p_2}{\partial x^2} + \alpha_2{}^2 p_1 - \alpha_3{}^2 p_2 \qquad (4)$$

Received: January 18, 2011
Revised: March 29, 2011
Published: April 11, 2011

$$\frac{1}{D}\frac{\partial p_3}{\partial t} = \frac{\partial^2 p_3}{\partial x^2} + \alpha_3{}^2 p_2 \quad (5)$$

D is the diffusion coefficient of all compounds; t is the time; $\alpha_i = (V_{\max(i)}/K_{m(i)}D)^{1/2}$, where i = 1, 2, and 3; $K_{m(i)}$ denote Michaelis−Menten constants; $V_{\max(i)}$ denote the maximal enzymatic rates. The initial and boundary conditions are

$$t = 0, \quad s_1 = s_0, \quad p_1 = 0, \quad p_2 = 0, \quad p_3 = 0 \quad (6a)$$

$$x = d, \quad s_1 = s_0, \quad p_1 = 0, \quad p_2 = 0, \quad p_3 = 0 \quad (6b)$$

$$x = 0, \quad \frac{\partial s_1}{\partial x} = 0, \quad \frac{\partial p_1}{\partial x} = 0, \quad \frac{\partial p_2}{\partial x} = 0, \quad \frac{\partial p_3}{\partial x} = 0 \quad (6c)$$

where d is the membrane thickness. The biosensor current i is defined by the following expression:

$$i = 2FD\left(\frac{\partial p_3}{\partial x}\right)_{x=0} \quad (7)$$

where F is the Faraday number.

■ ANALYTICAL SOLUTIONS FOR THE CONCENTRATION AND CURRENT OF COMPOUNDS IN TRIENZYME MEMBRANE

Using Laplace transformation in the partial differential equations eqs 2−5 and the condition eq 6a, the following differential equations in Laplace space are obtained:

$$\frac{d^2\bar{s}_1}{dx^2} - \alpha_1{}^2\bar{s}_1 - \frac{s}{D}\bar{s}_1 + \frac{s_0}{D} = 0 \quad (8)$$

$$\frac{d^2\bar{p}_1}{dx^2} + \alpha_1{}^2\bar{s}_1 - \alpha_2{}^2\bar{p}_1 - \frac{s}{D}\bar{p}_1 = 0 \quad (9)$$

$$\frac{d^2\bar{p}_2}{dx^2} + \alpha_2{}^2\bar{p}_1 - \alpha_3{}^2\bar{p}_2 - \frac{s}{D}\bar{p}_2 = 0 \quad (10)$$

$$\frac{d^2\bar{p}_3}{dx^2} + \alpha_3{}^2\bar{p}_2 - \frac{s}{D}\bar{p}_3 = 0 \quad (11)$$

Now the boundary conditions become

$$x = d, \quad \bar{s}_1 = \frac{s_0}{s}; \quad \bar{p}_1 = 0; \quad \bar{p}_2 = 0; \quad \bar{p}_3 = 0 \quad (12a)$$

$$x = 0, \quad \frac{d\bar{s}_1}{dx} = 0; \quad \frac{d\bar{p}_1}{dx} = 0; \quad \frac{d\bar{p}_2}{dx} = 0; \quad \bar{p}_3 = 0 \quad (12b)$$

where s is the Laplace variable and an overbar indicates a Laplace-transformed quantity. The set of expressions presented in eqs 8−11 defines the initial and boundary value problem in Laplace space. The analytical solutions (see Appendix A) of eqs 2−5 are

$$s_1 = \frac{s_0\cosh(\alpha_1 x)}{\cosh(\alpha_1 d)} + \frac{4s_0\alpha_1{}^2}{\pi}\sum_{n=0}^{\infty}\frac{\cos(lx)\exp(-(\alpha_1{}^2 + l^2)Dt)}{(-1)^n(2n+1)(\alpha_1{}^2 + l^2)} \quad (13)$$

$$p_1 = \frac{s_0\alpha_1{}^2}{\alpha_1{}^2 - \alpha_2{}^2}\left[\frac{\cosh(\alpha_2 x)}{\cosh(\alpha_2 d)} - \frac{\cosh(\alpha_1 x)}{\cosh(\alpha_1 d)}\right]$$
$$- \frac{4s_0\alpha_1{}^4}{\pi(\alpha_1{}^2 - \alpha_2{}^2)}\sum_{n=0}^{\infty}\frac{\cos(lx)\exp(-(\alpha_1{}^2 + l^2)Dt)}{(-1)^n(2n+1)(\alpha_1{}^2 + l^2)}$$
$$- \frac{4s_0\alpha_1{}^2}{\pi}\sum_{n=0}^{\infty}\frac{\cos(lx)\exp(-(\alpha_2{}^2 + l^2)Dt)}{(-1)^n(2n+1)(\alpha_2{}^2 - \alpha_1{}^2 + l^2)}$$
$$+ \frac{s_0\alpha_1{}^4\pi}{d^2(\alpha_1{}^2 - \alpha_2{}^2)}\sum_{n=0}^{\infty}\frac{(2n+1)\cos(lx)\exp(-(\alpha_2{}^2 + l^2)Dt)}{(-1)^n(\alpha_2{}^2 - \alpha_1{}^2 + l^2)} \quad (14)$$

$$p_2 = \frac{s_0\alpha_1{}^2\alpha_2{}^2\cosh(\alpha_3 x)}{(\alpha_3{}^2 - \alpha_1{}^2)(\alpha_3{}^2 - \alpha_2{}^2)\cosh(\alpha_3 d)}$$
$$+ \frac{4s_0\alpha_1{}^4\alpha_2{}^2}{(\alpha_1{}^2 - \alpha_2{}^2)(\alpha_1{}^2 - \alpha_3{}^2)\pi}\sum_{n=0}^{\infty}\frac{\cos(lx)\exp(-(\alpha_1{}^2 + l^2)Dt)}{(-1)^n(2n+1)(\alpha_1{}^2 + l^2)}$$
$$+ \frac{s_0\alpha_1{}^2\alpha_2{}^2\cosh(\alpha_2 x)}{(\alpha_2{}^2 - \alpha_1{}^2)(\alpha_2{}^2 - \alpha_3{}^2)\cosh(\alpha_2 d)}$$
$$+ \frac{s_0\alpha_1{}^4\alpha_2{}^2\pi}{(\alpha_1{}^2 - \alpha_3{}^2)(\alpha_2{}^2 - \alpha_3{}^2)d^2}\sum_{n=0}^{\infty}\frac{(2n+1)\cos(lx)\exp(-(\alpha_3{}^2 + l^2)Dt)}{(-1)^n(\alpha_3{}^2 + l^2)(\alpha_3{}^2 - \alpha_1{}^2 + l^2)}$$
$$+ \frac{s_0\alpha_1{}^2\alpha_2{}^2\cosh(\alpha_1 x)}{(\alpha_1{}^2 - \alpha_2{}^2)(\alpha_1{}^2 - \alpha_3{}^2)\cosh(\alpha_1 d)}$$
$$- \frac{s_0\alpha_1{}^4\alpha_2{}^2\pi}{(\alpha_1{}^2 - \alpha_2{}^2)(\alpha_2{}^2 - \alpha_3{}^2)d^2}\sum_{n=0}^{\infty}\frac{(2n+1)\cos(lx)\exp(-(\alpha_2{}^2 + l^2)Dt)}{(-1)^n(\alpha_2{}^2 + l^2)(\alpha_2{}^2 - \alpha_1{}^2 + l^2)}$$
$$+ \frac{4s_0\alpha_1{}^2\alpha_2{}^2}{\pi}\sum_{n=0}^{\infty}\frac{(-1)^n\cos(lx)\exp(-(\alpha_3{}^2 + l^2)Dt)}{(2n+1)(\alpha_3{}^2 - \alpha_1{}^2 + l^2)(\alpha_3{}^2 - \alpha_2{}^2 + l^2)}$$
$$+ \frac{4s_0\alpha_1{}^2\alpha_2{}^2}{(\alpha_2{}^2 - \alpha_3{}^2)\pi}\sum_{n=0}^{\infty}\frac{\cos(lx)\exp(-(\alpha_2{}^2 + l^2)Dt)}{(-1)^n(2n+1)(\alpha_2{}^2 - \alpha_1{}^2 + l^2)}$$
$$- \frac{s_0\alpha_1{}^2\alpha_2{}^2\pi}{(\alpha_2{}^2 - \alpha_3{}^2)d^2}\sum_{n=0}^{\infty}\frac{(2n+1)\cos(lx)\exp(-(\alpha_3{}^2 + l^2)Dt)}{(-1)^n(\alpha_3{}^2 - \alpha_1{}^2 + l^2)(\alpha_3{}^2 - \alpha_2{}^2 + l^2)} \quad (15)$$

$$p_3 = \frac{s_0\alpha_1{}^2\alpha_2{}^2(1 - \cosh(\alpha_3 x))}{(\alpha_3{}^2 - \alpha_1{}^2)(\alpha_3{}^2 - \alpha_2{}^2)\cosh(\alpha_3 d)}$$
$$+ \frac{2s_0\alpha_1{}^4\alpha_2{}^2}{\pi(\alpha_1{}^2 - \alpha_3{}^2)(\alpha_2{}^2 - \alpha_3{}^2)}\sum_{n=1}^{\infty}\frac{(-1)^n\sin(m(d-x))\exp(-m^2Dt)}{n(\alpha_1{}^2 - m^2)\cosh(\sqrt{\alpha_3{}^2 - m^2}d)}$$
$$- \frac{s_0\alpha_1{}^2\alpha_3{}^2(1 - \cosh(\alpha_2 x))}{(\alpha_1{}^2 - \alpha_2{}^2)(\alpha_2{}^2 - \alpha_3{}^2)\cosh(\alpha_2 d)}$$
$$- \frac{2s_0\alpha_1{}^4\alpha_3{}^2}{\pi(\alpha_1{}^2 - \alpha_2{}^2)(\alpha_2{}^2 - \alpha_3{}^2)}\sum_{n=1}^{\infty}\frac{(-1)^n\sin(m(d-x))\exp(-m^2Dt)}{n(\alpha_1{}^2 - m^2)\cosh(\sqrt{\alpha_2{}^2 - m^2}d)}$$
$$+ \frac{s_0\alpha_2{}^2\alpha_3{}^2(1 - \cosh(\alpha_1 x))}{(\alpha_1{}^2 - \alpha_2{}^2)(\alpha_1{}^2 - \alpha_3{}^2)\cosh(\alpha_1 d)}$$
$$+ \frac{2s_0\alpha_1{}^2\alpha_2{}^2\alpha_3{}^2}{\pi(\alpha_1{}^2 - \alpha_2{}^2)(\alpha_1{}^2 - \alpha_3{}^2)}\sum_{n=1}^{\infty}\frac{(-1)^n\sin(m(d-x))\exp(-m^2Dt)}{n(\alpha_1{}^2 - m^2)\cosh(\sqrt{\alpha_1{}^2 - m^2}d)}$$
$$+ \frac{s_0\alpha_1{}^2\alpha_2{}^2 x}{d(\alpha_3{}^2 - \alpha_1{}^2)(\alpha_3{}^2 - \alpha_2{}^2)}\left(1 - \frac{1}{\cosh(\alpha_3 d)}\right)$$

$$+\frac{2s_0{\alpha_1}^2{\alpha_2}^2\pi}{({\alpha_2}^2-{\alpha_3}^2)d^2}\sum_{n=1}^{\infty}\frac{n(-1)^n\sin(m(d-x))\exp(-m^2Dt)}{({\alpha_1}^2-m^2)({\alpha_2}^2-m^2)\cosh(\sqrt{{\alpha_3}^2-m^2}d)}$$

$$-\frac{s_0{\alpha_1}^2{\alpha_3}^2x}{d({\alpha_1}^2-{\alpha_2}^2)({\alpha_2}^2-{\alpha_3}^2)}\left(1-\frac{1}{\cosh(\alpha_2 d)}\right)$$

$$-\frac{2s_0{\alpha_1}^2{\alpha_3}^2\pi}{({\alpha_2}^2-{\alpha_3}^2)d^2}\sum_{n=1}^{\infty}\frac{n(-1)^n\sin(m(d-x))\exp(-m^2Dt)}{({\alpha_1}^2-m^2)({\alpha_2}^2-m^2)\cosh(\sqrt{{\alpha_2}^2-m^2}d)}$$

$$+\frac{s_0{\alpha_2}^2{\alpha_3}^2x}{d({\alpha_1}^2-{\alpha_2}^2)({\alpha_1}^2-{\alpha_3}^2)}\left(1-\frac{1}{\cosh(\alpha_1 d)}\right)$$

$$-\frac{2s_0{\alpha_1}^2{\alpha_2}^2{\alpha_3}^2}{\pi}\sum_{n=1}^{\infty}\frac{(\sin(mx)+\sin(m(d-x)))\exp(-m^2Dt)}{n(-1)^n({\alpha_1}^2-m^2)({\alpha_2}^2-m^2)({\alpha_3}^2-m^2)}$$

$$+\left(\frac{2s_0{\alpha_1}^2{\alpha_2}^2}{\pi({\alpha_3}^2-{\alpha_1}^2)({\alpha_3}^2-{\alpha_2}^2)}-\frac{2s_0{\alpha_1}^2{\alpha_3}^2}{\pi({\alpha_1}^2-{\alpha_2}^2)({\alpha_2}^2-{\alpha_3}^2)}\right.$$

$$\left.+\frac{2s_0{\alpha_2}^2{\alpha_3}^2}{\pi({\alpha_1}^2-{\alpha_2}^2)({\alpha_1}^2-{\alpha_3}^2)}\right)\sum_{n=1}^{\infty}\frac{(\sin(mx)\exp(-m^2Dt)}{n(-1)^n({\alpha_1}^2-m^2)}$$

$$+\frac{2s_0{\alpha_1}^2\pi}{d^2}\sum_{n=1}^{\infty}\frac{n\sin(mx)\exp(-m^2Dt)}{(-1)^n({\alpha_1}^2-m^2)({\alpha_2}^2-m^2)}$$

$$+\frac{2s_0{\alpha_1}^2{\alpha_2}^2\pi}{d^2}\sum_{n=1}^{\infty}\frac{(-1)^n n\sin(mx)\exp(-m^2Dt)}{({\alpha_1}^2-m^2)({\alpha_2}^2-m^2)({\alpha_3}^2-m^2)}$$

$$+\frac{2s_0{\alpha_1}^2{\alpha_2}^2\pi}{d^2}\sum_{n=1}^{\infty}\frac{n(-1)^n\sin(m(d-x))\exp(-m^2Dt)}{({\alpha_1}^2-m^2)({\alpha_2}^2-m^2)({\alpha_2}^2-m^2)\cosh(\sqrt{{\alpha_3}^2-m^2}d)} \tag{16}$$

When time tends to infinity, the analytical expression of non-steady-state concentration (eqs 13−16) approaches the steady-state value, thereby confirming the validity of the mathematical analysis. The biosensor current i is

$$i=2FD\left\{\frac{2s_0{\alpha_1}^2{\alpha_2}^2\pi^2}{d^3}\sum_{n=1}^{\infty}\frac{n^2(-1)^n\exp(-m^2Dt)}{({\alpha_1}^2-m^2)({\alpha_2}^2-m^2)({\alpha_3}^2-m^2)}\right.$$

$$-\frac{2s_0{\alpha_1}^2{\alpha_2}^2{\alpha_3}^2}{d({\alpha_1}^2-{\alpha_2}^2)({\alpha_1}^2-{\alpha_3}^2)}\sum_{n=1}^{\infty}\frac{\exp(-m^2Dt)}{({\alpha_1}^2-m^2)\cosh(\sqrt{{\alpha_1}^2-m^2}d)}$$

$$+\frac{2s_0{\alpha_1}^2{\alpha_2}^2{\alpha_3}^2}{d}\sum_{n=1}^{\infty}\frac{((-1)^n-1)\exp(-m^2Dt)}{({\alpha_1}^2-m^2)({\alpha_2}^2-m^2)({\alpha_3}^2-m^2)}$$

$$+\frac{2s_0{\alpha_1}^2{\alpha_3}^2\pi^2}{d^3({\alpha_2}^2-{\alpha_3}^2)}\sum_{n=1}^{\infty}\frac{n^2\exp(-m^2Dt)}{({\alpha_1}^2-m^2)({\alpha_2}^2-m^2)\cosh(\sqrt{{\alpha_1}^2-m^2}d)}$$

$$+\frac{s_0{\alpha_1}^2{\alpha_2}^2}{d({\alpha_3}^2-{\alpha_1}^2)({\alpha_3}^2-{\alpha_2}^2)}\left(1-\frac{1}{\cosh(\alpha_3 d)}\right)$$

$$-\frac{2s_0{\alpha_1}^2{\alpha_2}^2\pi^2}{d^3({\alpha_2}^2-{\alpha_3}^2)}\sum_{n=1}^{\infty}\frac{n^2\exp(-m^2Dt)}{({\alpha_1}^2-m^2)({\alpha_2}^2-m^2)\cosh(\sqrt{{\alpha_1}^2-m^2}d)}$$

$$-\frac{s_0{\alpha_1}^2{\alpha_3}^2}{d({\alpha_1}^2-{\alpha_2}^2)({\alpha_2}^2-{\alpha_3}^2)}\left(1-\frac{1}{\cosh(\alpha_2 d)}\right)$$

$$+\frac{2s_0{\alpha_1}^4{\alpha_3}^2}{d({\alpha_1}^2-{\alpha_2}^2)({\alpha_2}^2-{\alpha_3}^2)}\sum_{n=1}^{\infty}\frac{\exp(-m^2Dt)}{({\alpha_1}^2-m^2)\cosh(\sqrt{{\alpha_2}^2-m^2}d)}$$

$$+\frac{s_0{\alpha_2}^2{\alpha_3}^2}{d({\alpha_1}^2-{\alpha_2}^2)({\alpha_1}^2-{\alpha_3}^2)}\left(1-\frac{1}{\cosh(\alpha_1 d)}\right)$$

$$+\left[\frac{2s_0{\alpha_1}^4{\alpha_2}^2}{d({\alpha_1}^2-{\alpha_3}^2)({\alpha_2}^2-{\alpha_3}^2)}-\frac{2s_0{\alpha_1}^4{\alpha_3}^2}{d({\alpha_1}^2-{\alpha_2}^2)({\alpha_2}^2-{\alpha_3}^2)}\right.$$

$$\left.+\frac{2s_0{\alpha_1}^2{\alpha_2}^2{\alpha_3}^2}{d({\alpha_1}^2-{\alpha_2}^2)({\alpha_1}^2-{\alpha_3}^2)}\right]\sum_{n=1}^{\infty}\frac{(-1)^n\exp(-m^2Dt)}{{\alpha_1}^2-m^2}$$

$$+\frac{2s_0{\alpha_1}^2\pi^2}{d^3}\sum_{n=1}^{\infty}\frac{n^2(-1)^n\exp(-m^2Dt)}{({\alpha_1}^2-m^2)({\alpha_2}^2-m^2)}$$

$$\left.-\frac{2s_0{\alpha_1}^2{\alpha_2}^2\pi^2}{d^3}\sum_{n=1}^{\infty}\frac{n^2\exp(-m^2Dt)}{({\alpha_1}^2-m^2)({\alpha_2}^2-m^2)({\alpha_3}^2-m^2)\cosh(\sqrt{{\alpha_3}^2-m^2}d)}\right\} \tag{17}$$

where

$$l=\frac{(2n+1)\pi}{d}\qquad\text{and}\qquad m=\frac{n\pi}{d} \tag{18}$$

When $t\rightarrow\infty$, the steady-state current was obtained from eq 17 and is shown by

$$i=2FD\left\{\frac{s_0{\alpha_1}^2{\alpha_2}^2}{d({\alpha_3}^2-{\alpha_1}^2)({\alpha_3}^2-{\alpha_2}^2)}\left(1-\frac{1}{\cosh(\alpha_3 d)}\right)\right.$$

$$-\frac{s_0{\alpha_1}^2{\alpha_3}^2}{d({\alpha_2}^2-{\alpha_1}^2)({\alpha_3}^2-{\alpha_2}^2)}\left(1-\frac{1}{\cosh(\alpha_2 d)}\right)$$

$$\left.+\frac{s_0{\alpha_2}^2{\alpha_3}^2}{d(\alpha_1^2-{\alpha_2}^2)({\alpha_1}^2-{\alpha_3}^2)}\left(1-\frac{1}{\cosh(\alpha_1 d)}\right)\right\} \tag{19}$$

This steady-state current is same as the result of the work of Kulys [see eq 7 of ref 16].

NUMERICAL SIMULATION

The diffusion equations [eqs 2−5] for the boundary conditions [eqs 6a−6c] are solved by numerical methods. The function pdex4 in Matlab software, which is a function of solving the initial boundary value problems for partial differential equations, was used to solve these equations. Its numerical solution is compared with our analytical results in Figure 1, and it gives a excellent agreement for all values of time t and diffusion modules $\alpha_1 d$, $\alpha_2 d$, and $\alpha_3 d$ in a trienzyme membrane. The Matlab program is also given in Appendix C.

DISCUSSION

Figure 1 represents the non-steady-state concentration profiles in enzyme membrane of biosensor. Figure 1a shows the concentration s_1 versus membrane thickness x in trienzyme membrane for various values of time t and for diffusion modules $\alpha_1 d$, $\alpha_2 d$, and $\alpha_3 d$. From Figure 1a, it is evident that the value of the concentration $s_1 \approx 1$ when $x = 0.01$. The value of the concentration s_1 decreases when time increases. The concentration reaches the steady-state value when $t \geq 10$. Figure 1b represents the concentration p_1 versus membrane thickness x in trienzyme membrane for various values of time t and for diffusion modules $\alpha_1 d$, $\alpha_2 d$, and $\alpha_3 d$. From Figure 1b, it is inferred that when $x \leq 0.004$, all the curves reach the

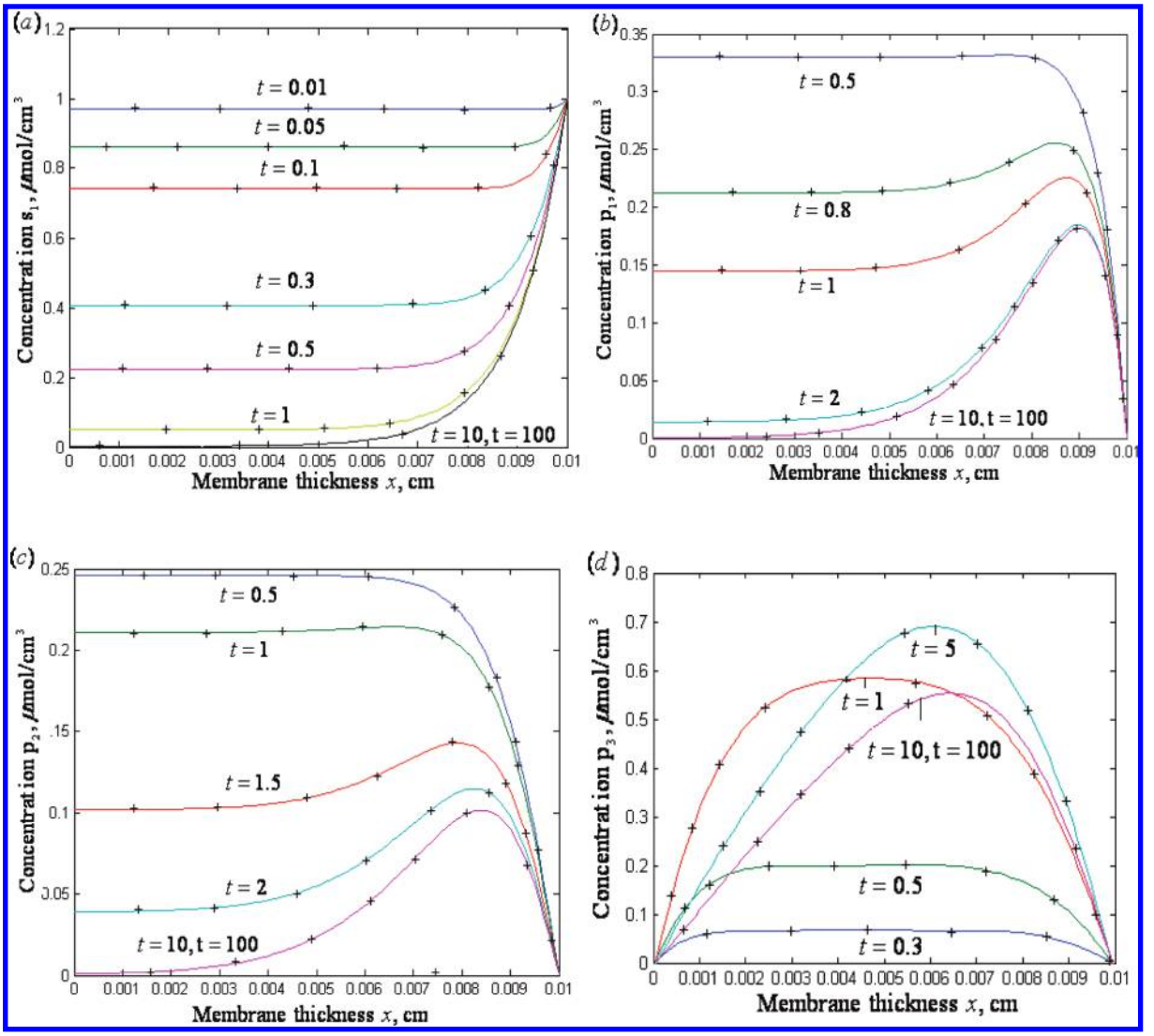

Figure 1. Concentration profiles for (a) concentration s_1, (b) concentration p_1, (c) concentration p_2, and (d) concentration p_3 in trienzyme membrane for various values of time t when s_0 = 1 μmol/cm^3, d = 0.01 cm, and for diffusion modules $\alpha_1 d$ = 10.0, $\alpha_2 d$ = 10.1, and $\alpha_3 d$ = 10.3. Symbols: (—) eqs 13−16; (+) numerical simulation.

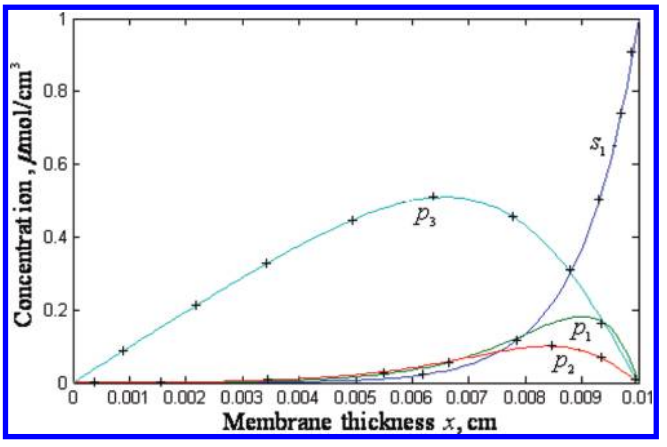

Figure 2. Plot of compound concentration versus membrane thickness x in trienzyme membrane. The concentrations were computed using eqs 13−16 for s_0 = 1 μmol/cm^3, $\alpha_1 d$ = 10.0, $\alpha_2 d$ = 10.1, $\alpha_3 d$ = 10.3, d = 0.01 cm, and time $t \geq 10$. Symbols: (—) eqs 13−16; (+) Figure 1 of ref 16.

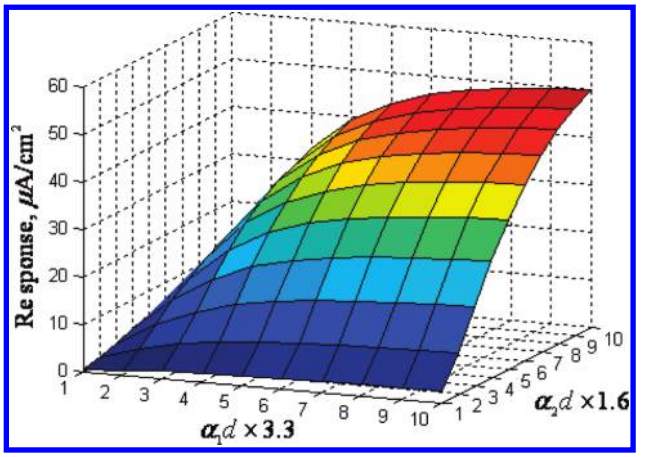

Figure 3. Plot of the three-dimensional current i calculated using eqs 17 and 19 for s_0 = 1 μmol/cm^3, $\alpha_3 d$ = 10.3, and $t \geq 100$.

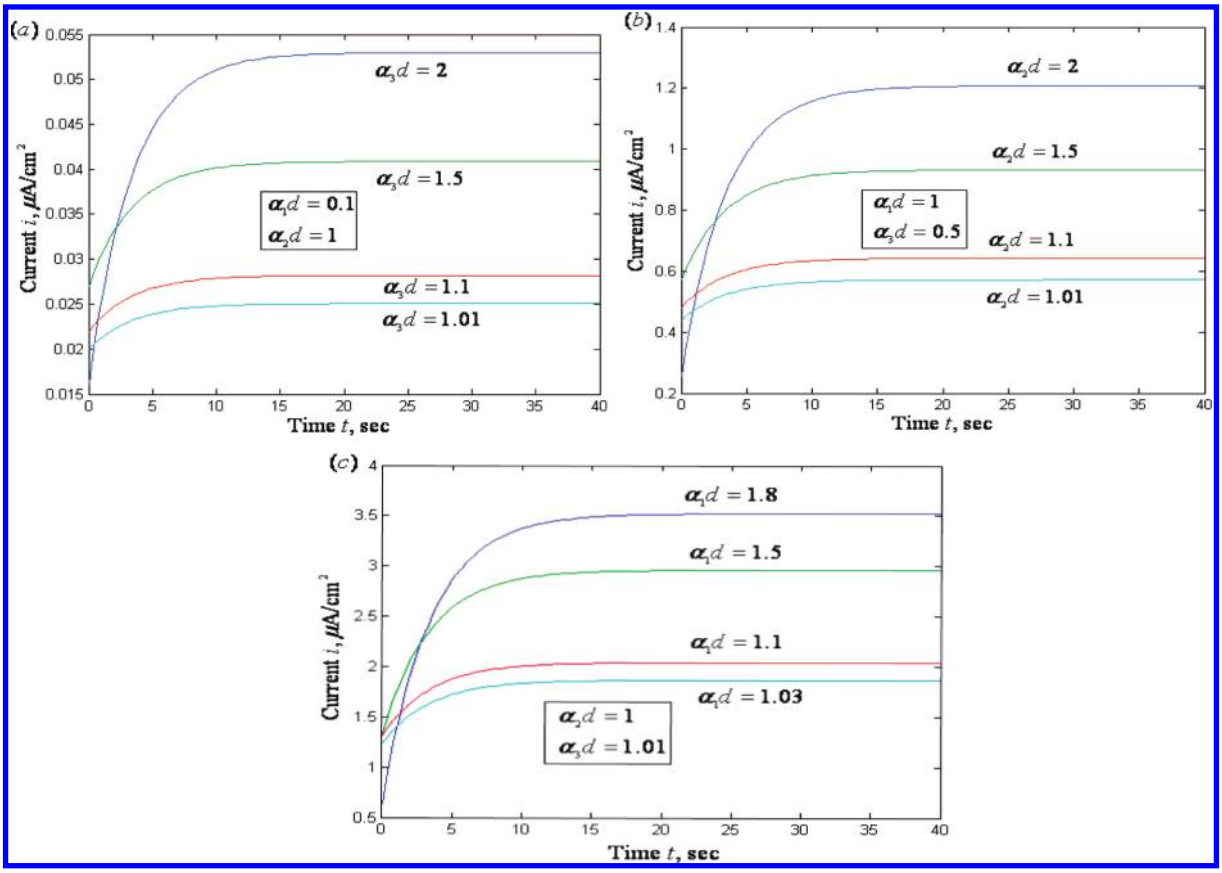

Figure 4. Biosensor current i plotted as a function of time t. The biosensor currents were computed using eq 17 when $s_0 = 1\ \mu\text{mol/cm}^3$ for (a) fixed values of $\alpha_1 d = 0.1$ and $\alpha_2 d = 1$ and various values of $\alpha_3 d$, (b) fixed values of $\alpha_1 d = 1$ and $\alpha_3 d = 0.5$ and various values of $\alpha_2 d$, and (c) fixed values of $\alpha_2 d = 1$ and $\alpha_3 d = 1.01$ and various values of $\alpha_1 d$.

steady-state value. A series of non-steady-state concentrations p_2 for various values of time t is plotted in Figure 1c. From Figure 1c, it is obvious that there is a simultaneous decrease in the values of concentration p_2 and the steady-state value is reached when $t \geq 10$. The non-steady-state concentration p_3 for various values of time t and for diffusion modules $\alpha_1 d$, $\alpha_2 d$, and $\alpha_3 d$ is plotted in Figure 1d. From Figure 1d, it is evident that initially the value of the concentration increases and reaches the maximum value when $x = 0.006$ and $t = 5$. The value of the concentration p_3 becomes zero when $x = 0$ and $x = 0.01$. Figure 2 represents the non-steady-state concentrations s_1, p_1, p_2, and p_3 versus membrane thickness x in trienzyme membrane for various values of time t and for diffusion modules $\alpha_1 d$, $\alpha_2 d$, and $\alpha_3 d$. In Figure 2, our non-steady-state analytical results [eqs 13−16] are compared with steady-state results when $t \geq 10$, and further when $x \geq 0.006$ the value of concentration s_1 increases and reaches the value 1. The value of the concentration p_1 increases when $x \geq 0.004$ and decreases gradually to reach the value 0.01. The value of the concentration p_2 increases when $x \geq 0.004$ and decreases gradually to reach the value 0.01. The value of the concentration p_3 increases and attains the maximum value when $0.006 \leq x \leq 0.007$ and then decreases gradually.

Figure 3 represents a three-dimensional current i calculated using eqs 17 and 19 for $s_0 = 1\ \mu\text{mol/cm}^3$, $\alpha_3 d = 10.3$, and $t \geq 100$. Figure 3 compares the biosensor response i obtained in this work with Kulys's work.[16] Upon comparison, it is evident that both results are identical. Figure 4 indicates the non-steady-state current response i for various values of diffusion modules $\alpha_1 d$, $\alpha_2 d$, and $\alpha_3 d$. Figure 4a represents the current i for all values of $\alpha_3 d$ [=1.01, 1.1, 1.5, 2] when $\alpha_1 d = 0.1$ and $\alpha_2 d = 1$ using eq 17. From Figure 4a, it is evident that i increases when $\alpha_3 d$ increases. Furthermore, when $t \geq 20$, all the curves reach the steady-state value. Figure 4b indicates the current i for all values of $\alpha_2 d$ [=1.01, 1.1, 1.5, 2] when $\alpha_1 d = 1$ and $\alpha_3 d = 0.5$ using eq 17. From Figure 4b, it is evident that i increases when $\alpha_2 d$ increases. Also, when $t \geq 20$, all the curves reach the steady-state value. Figure 4c indicates the current i for all values of $\alpha_1 d$ [=1.03, 1.1, 1.5, 1.8] when $\alpha_2 d = 1$ and $\alpha_3 d = 1.01$ using eq 17. From Figure 4c, it is evident that i increases when $\alpha_3 d$ increases. Also, when $t \geq 20$, all the curves reach the steady-state value.

CONCLUSIONS

In this work, we obtained an analytical solution for a biosensor containing three immobilized enzymes utilizing consecutive substrate conversion. An amperometric trienzyme biosensor electrode was constructed for the determination of creatine and creatinine in pharmaceutical products and serum samples. The response characteristics of the electrodes are measured at different potentials to determine the appropriate working potential (higher sensitivity, lower limit of detection, wide linear concentration range, etc.) for the simultaneous detection of creatine and creatinine. Time-dependent linear diffusion equations have been formulated and solved analytically. The analytical expressions for the concentrations and

dx.doi.org/10.1021/jp200520s |J. Phys. Chem. A 2011, 115, 4299–4306

current for catalytic reactions with diffusion coefficient at trienzyme membrane under non-steady-state conditions are obtained by using the complex inversion formula. An excellent agreement with the existing steady-state result is noted. Furthermore, the numerical simulation was in excellent agreement with the analytically obtained concentration and current.

APPENDIX A

Solution of eqs 8−11 Using Complex Inversion Formula. In this appendix we indicate how eqs 13−16 are derived. By solving a differential equation of second order with constant coefficients, we obtained the solution of the eq 8 as

$$\bar{s}_1 = \frac{s_0 \alpha_1{}^2 D \cosh\left(\sqrt{\alpha_1^2 + \frac{s}{D}}\, x\right)}{s(s + \alpha_1{}^2 D) \cosh\left(\sqrt{\alpha_1{}^2 + \frac{s}{D}}\, d\right)} + \frac{s_0}{s + \alpha_1{}^2 D} \quad \text{(A1)}$$

In this appendix we indicate how eq A1 may be inverted using the complex inversion formula. If $\bar{y}(s)$ represents the Laplace transform of a function $y(\tau)$, then according to the complex inversion formula we can state that

$$y(\tau) = \frac{1}{2\pi i}\int_{c-i\infty}^{c+i\infty} \exp[s\tau]\, \bar{y}(s)\, ds = \frac{1}{2\pi i}\oint_c \exp[s\tau]\, \bar{y}(s)\, ds \quad \text{(A2)}$$

where the integration in eq A2 is to be performed along a line $s = c$ in the complex plane where $s = x + iy$. The real number c is chosen such that $s = c$ lies to the right of all the singularities, but is otherwise assumed to be arbitrary. In practice, the integral is evaluated by considering the contour integral presented on the right-hand side of eq A2, which is evaluated using the so-called Bromwich contour. The contour integral is then evaluated using the residue theorem which states for any analytic function $F(z)$

$$\oint_c F(z)\, dz = 2\pi i \sum_n \text{Re } s[F(z)]_{z=z_n} \quad \text{(A3)}$$

where the residues are computed at the poles of the function $F(z)$. Hence from eq A3, we note that

$$y(\tau) = \sum_n \text{Re } s[\exp[s\tau]\, \bar{y}(s)]_{s=s_n} \quad \text{(A4)}$$

From the theory of complex variables we can show that the residue of a function $F(z)$ at a simple pole at $z = a$ is given by

$$\text{Re } s[F(z)]_{z=a} = \lim_{z \to a}\{(z-a)F(z)\} \quad \text{(A5)}$$

Hence in order to invert eq A1, we need to evaluate

$$\text{Re } s\left[\frac{\cosh\left(\sqrt{\alpha_1{}^2 + \frac{s}{D}}\, x\right)}{s(s + \alpha_1{}^2 D) \cosh\left(\sqrt{\alpha_1{}^2 + \frac{s}{D}}\, d\right)}\right]$$

Now the poles are obtained from

$$s(s + \alpha_1{}^2 D) \cosh\left(\sqrt{\alpha_1{}^2 + \frac{s}{D}}\, d\right) = 0$$

Hence there is a simple pole at $s = 0$ and there is a pole at $s = -\alpha_1{}^2 D$, and there are infinitely many poles given by the solution of the equation

$$\cosh\left(\sqrt{\alpha_1{}^2 + \frac{s}{D}}\, d\right) = 0$$

and so

$$s_n = -\alpha_1{}^2 - \frac{(2n+1)^2 \pi^2}{4d^2} \qquad \text{with } n = 0, 1, 2, \ldots$$

Hence we note that

$$S(X,T) = \text{Re } s\left[\frac{\cosh\left(\sqrt{\alpha_1{}^2 + \frac{s}{D}}\, x\right)}{s(s + \alpha_1{}^2 D) \cosh\left(\sqrt{\alpha_1{}^2 + \frac{s}{D}}\, d\right)}\right]_{s=0} + \text{Re } s\left[\frac{\cosh\left(\sqrt{\alpha_1{}^2 + \frac{s}{D}}\, x\right)}{s(s + \alpha_1{}^2 D) \cosh\left(\sqrt{\alpha_1{}^2 + \frac{s}{D}}\, d\right)}\right]_{s=s_n} \quad \text{(A6)}$$

The first residue in eq A6 is given by

$$\text{Re } s\left[\frac{\cosh\left(\sqrt{\alpha_1{}^2 + \frac{s}{D}}\, x\right)}{s(s + \alpha_1{}^2 D) \cosh\left(\sqrt{\alpha_1{}^2 + \frac{s}{D}}\, d\right)}\right]_{s=0} = \lim_{s \to 0}\left\{\frac{\exp(sT) \cosh\left(\sqrt{\alpha_1{}^2 + \frac{s}{D}}\, x\right)}{(s + \alpha_1{}^2 D) \cosh\left(\sqrt{\alpha_1{}^2 + \frac{s}{D}}\, d\right)}\right\} = \frac{\cosh(\alpha_1 x)}{\alpha_1{}^2 D \cosh(\alpha_1 d)} \quad \text{(A7)}$$

The second residue in eq A6 is as follows:

$$\text{Re } s\left[\frac{\cosh\left(\sqrt{\alpha_1{}^2 + \frac{s}{D}}\, x\right)}{s(s + \alpha_1{}^2 D) \cosh\left(\sqrt{\alpha_1{}^2 + \frac{s}{D}}\, d\right)}\right]_{s=0}$$

dx.doi.org/10.1021/jp200520s |J. Phys. Chem. A 2011, 115, 4299–4306

$$= \lim_{s \to -\alpha_1^2 D} \left\{ \frac{\exp(sT)\cosh\left(\sqrt{\alpha_1^2 + \frac{s}{D}}\,x\right)}{s\cosh\left(\sqrt{\alpha_1^2 + \frac{s}{D}}\,d\right)} \right\}$$
$$= \frac{-\exp(-\alpha_1^2 DT)}{\alpha_1^2 D} \quad \text{(A8)}$$

The third residue in eq A6 can be evaluated as follows. It is established that if $F(z)$ can be expressed as $F(z) = f(z)/g(z)$, where the functions f and g are analytic at $s = s_n$ and $g(s_n) = 0$ while $g'(s_n) \neq 0$ and $f(s_n) \neq 0$, then

$$\text{Re } s[F(z)]_{s=s_n} = \sum_{n=0}^{\infty} \frac{f(s_n)}{g'(s_n)} \exp[s\tau]$$

Hence we can show that

$$\underset{s \to s_n}{\text{Lt}}\, e^{st} \frac{\cosh\left(\sqrt{\alpha_1^2 + \frac{s}{D}}\,x\right)}{s(s + \alpha_1^2 D)\frac{d}{ds}\cosh\left(\sqrt{\alpha_1^2 + \frac{s}{D}}\,d\right)}$$
$$= \underset{s \to s_n}{\text{Lt}}\, e^{st} \frac{\cosh\left(\sqrt{\alpha_1^2 + \frac{s}{D}}\,x\right)\left[2D\sqrt{\alpha_1^2 + \frac{s}{D}}\right]}{s_n d(s + \alpha_1^2 D)\cosh\left(\sqrt{\alpha_1^2 + \frac{s}{D}}\,d\right)}$$

$$= \frac{2D\exp\left[-\left(\alpha_1^2 + \frac{(2n+1)^2\pi^2}{4d^2}\right)Dt\right]\left(i\frac{(2n+1)\pi}{2d}\right)\cosh\left(i\frac{(2n+1)\pi}{2d}x\right)}{d\left(\alpha_1^2 + \frac{(2n+1)^2\pi^2}{4d^2}\right)D\frac{(2n+1)^2\pi^2}{4d^2}D\sinh\left(i\frac{(2n+1)\pi}{2d}d\right)}$$

$$\text{for } = 0, 1, \ldots \quad \text{(A9)}$$

Using $\cosh(i\theta) = \cos(\theta)$ and $\sinh(i\theta) = i\sin(\theta)$

$$\underset{s \to s_n}{\text{Lt}}\, e^{st} \frac{\cosh\left(\sqrt{\alpha_1^2 + \frac{s}{D}}\,x\right)}{s(s + \alpha_1^2 D)\frac{d}{ds}\cosh\left(\sqrt{\alpha_1^2 + \frac{s}{D}}\,d\right)}$$
$$= \frac{4}{\pi D}\sum_{n=0}^{\infty} \frac{(-1)^n \cos\left(\frac{(2n+1)\pi}{2d}x\right)\exp\left[-\left(\alpha_1^2 + \frac{(2n+1)^2\pi^2}{4d^2}\right)Dt\right]}{(2n+1)\left(\alpha_1^2 + \frac{(2n+1)^2\pi^2}{4d^2}\right)} \quad \text{(A10)}$$

Similarly, we can invert eqs 9−11.

APPENDIX B

This appendix contains the Matlab program to find the sum of the series of eq 13.

```
function v=v(x)
alpha1=1000;
m=1;
d=0.01;
D=3*10^(-6);
x=linspace(0,0.01);
t=1;
s=0;
N=100;
for n=0: 1 :N+1;
s=s+(-1)^n*cos((2*n+1)*pi*x/(2*d))
*exp(-alpha1^2*D*t+(2*n+1)-
^2*pi^2*D*t/(4*d^2)))/
((2*n+1)*(alpha1^2+(2*n+1)^2*pi^2/(4*d^2)));
end
u=m*cosh(alpha1*x)/cosh(alpha1*d);
v=u+4*m*alpha1^2/pi*s;
plot(x,v)
```

Similarly, we can find the sum of the series of eqs 14−16.

APPENDIX C

The Matlab program to find the numerical solution of eqs 2−5 is as follows.

```
function pdex4
m=0;
x=linspace(0,0.01);
t=linspace(0,0.5);
sol=pdepe(m,@pdex4pde,@pdex4ic,@pdex4bc,x,t);
u1=sol(:,:,1);
u2=sol(:,:,2);
u3=sol(:,:,3);
u4=sol(:,:,4);
figure
plot(x,u1(end,:))
title('u1(x,t)')
figure
plot(x,u2(end,:))
title('u2(x,t)')
figure
plot(x,u3(end,:))
title('u3(x,t)')
figure
plot(x,u4(end,:))
title('u4(x,t)')
% --------------------------------------------------------------
function [c,f,s]=pdex4pde(x,t,u,DuDx)
D=3*10^(-6);
alpha1=1000;
alpha2=1010;
alpha3=1030;
c=[1/D; 1/D; 1/D; 1/D];
f=[1; 1; 1; 1].* DuDx;
F1=-alpha1^2*u(1);
F2=alpha1^2*u(1)-alpha2^2*u(2);
F3=alpha2^2*u(2)-alpha3^2*u(3);
F4=alpha3^2*u(3);
s=[F1; F2; F3; F4];
% --------------------------------------------------------------
function u0=pdex4ic(x);
u0=[1; 0; 0; 0];
% --------------------------------------------------------------
function [pl,ql,pr,qr]=pdex4bc(xl,ul,xr,ur,t)
pl=[0; 0; 0; ul(4)];
ql=[1;1; 1; 0];
pr=[ur(1)-1; ur(2); ur(3); ur(4)];
qr=[0; 0; 0; 0];
```


dx.doi.org/10.1021/jp200520s |J. Phys. Chem. A 2011, 115, 4299–4306

AUTHOR INFORMATION

Corresponding Author
*Tel.: +91 9442228951. Fax: +91 0452 2675238. E-mail: raj_sms@rediffmail.com.

ACKNOWLEDGMENT

This work was supported by the CSIR, New Delhi, India. The authors are thankful to Dr. T. V. Krishnamoorthy, The Prinicipal, The Madura College, Madurai, and Mr. M. S. Meenakshisundaram, The Secretary, Madura College Board, Madurai, for their encouragement. We thank the reviewers for their valuable comments to improve the quality of the manuscript.

REFERENCES

(1) Guilbault, G. G. *Analytical Uses of Immobilized Enzymes*; Marcel Dekker: New York, 1984.
(2) *Biosensors: Fundamentals and Applications*; Turner, A. P. F., Karube, I., Wilson, G. S., Eds.; Oxford University Press: Oxford, U.K., 1987.
(3) Scheller, F.; Schubert, F. *Biosensors*; Elsevier: Amsterdam, 1992.
(4) Guilbault, G. G.; Nagy, G. *Anal. Chem.* **1973**, *45*, 417–419.
(5) Mell, L. D.; Maloy, J. T. *Anal. Chem.* **1975**, *47*, 299–307.
(6) Mell, L. D.; Maloy, J. T. *Anal. Chem.* **1976**, *48*, 1597–1601.
(7) Kulys, J. J.; Sorochinski, V. V.; Vidziunaite, R. A. *Biosensors* **1986**, *2*, 135–146.
(8) Schulmeister, T.; Rose, J.; Scheller, F. *Biosens. Bioelectron.* **1997**, *12*, 1021–1030.
(9) Schulmeister, T. *Sel. Electrode Rev.* **1990**, *12*, 203–260.
(10) Baronas, R.; Ivanauskas, F.; Kulys, J.; Sapagovas, M. *Nonlinear Anal.: Modell. Control* **2003**, *8*, 3–18.
(11) Baeumner, A. J.; Jones, C.; Wong, C. Y.; Price, A. *Anal. Bioanal. Chem.* **2004**, *378*, 1587–1593.
(12) Baronas, R.; Ivanauska, F.; Kulys, J. *Sensors* **2003**, *3*, 248–262.
(13) Velho, G. D.; Reach, G.; Thevenot, D. R. The design and development of in vivo glucose, sensors for an artificial endocrine pancreas. In *Biosensors: Fundamentals and Applications*; Turner, A. P. F., Karube, I., Wilson, G. S., Eds.; Oxford University Press: New York, 1987.
(14) Whitaker, J. R. The need for biosensors in the food industry and food research. In *Food Biosensor Analysis*; Wagner, G., Guilbault, G. G., Eds.; Marcel Dekker: New York, 1994.
(15) Stefan, R. I.; Bokretsion, R. G.; Staden, J. F.; Aboul-Enein, H. Y. *Talanta* **2003**, *60*, 1223–1228.
(16) Kulys, J. *Nonlinear Anal.: Modell. Control* **2004**, *9*, 139–144.